10-2017

The Trophic Life Cycle Stage of the Opportunistic Fungal Pathogen *Pneumocystis murina* Hinders the Ability of Dendritic Cells to Stimulate CD4$^+$ T Cell Responses

Heather M. Evans
University of Kentucky, heather.evans@uky.edu

Andrew Simpson
University of Kentucky, atsi224@uky.edu

Shu Shen
University of Kentucky, shu.shen@uky.edu

Arnold J. Stromberg
University of Kentucky, stromberg@uky.edu

Carol L. Pickett
University of Kentucky, cpicket@email.uky.edu

See next page for additional authors

Authors
Heather M. Evans, Andrew Simpson, Shu Shen, Arnold J. Stromberg, Carol L. Pickett, and Beth A. Garvy

The Trophic Life Cycle Stage of the Opportunistic Fungal Pathogen *Pneumocystis murina* Hinders the Ability of Dendritic Cells to Stimulate CD4$^+$ T Cell Responses

Notes/Citation Information
Published in *Infection and Immunity*, v. 85, issue 10, e00396-17, p. 1-16.

Digital Object Identifier (DOI)
https://doi.org/10.1128/IAI.00396-17

AMERICAN SOCIETY FOR MICROBIOLOGY | Infection and Immunity®

FUNGAL AND PARASITIC INFECTIONS

The Trophic Life Cycle Stage of the Opportunistic Fungal Pathogen *Pneumocystis murina* Hinders the Ability of Dendritic Cells To Stimulate CD4$^+$ T Cell Responses

Heather M. Evans,[a] Andrew Simpson,[a] Shu Shen,[b]* Arnold J. Stromberg,[b] Carol L. Pickett,[a] Beth A. Garvy[a,c]

Department of Microbiology, Immunology, and Molecular Genetics,[a] Department of Statistics,[b] and Division of Infectious Diseases, Department of Internal Medicine,[c] University of Kentucky, Lexington, Kentucky, USA

ABSTRACT The life cycle of the opportunistic fungal pathogen *Pneumocystis murina* consists of a trophic stage and an ascus-like cystic stage. Infection with the cyst stage induces proinflammatory immune responses, while trophic forms suppress the cytokine response to multiple pathogen-associated molecular patterns (PAMPs), including β-glucan. A targeted gene expression assay was used to evaluate the dendritic cell response following stimulation with trophic forms alone, with a normal mixture of trophic forms and cysts, or with β-glucan. We demonstrate that stimulation with trophic forms downregulated the expression of multiple genes normally associated with the response to infection, including genes encoding transcription factors. Trophic forms also suppressed the expression of genes related to antigen processing and presentation, including the gene encoding the major histocompatibility complex (MHC) class II transactivator, CIITA. Stimulation of dendritic cells with trophic forms, but not a mixture of trophic forms and cysts, reduced the expression of MHC class II and the costimulatory molecule CD40 on the surface of the cells. These defects in the expression of MHC class II and costimulatory molecules corresponded with a reduced capacity for trophic form-loaded dendritic cells to stimulate CD4$^+$ T cell proliferation and polarization. These data are consistent with the delayed innate and adaptive responses previously observed in immunocompetent mice inoculated with trophic forms compared to responses in mice inoculated with a mixture of trophic forms and cysts. We propose that trophic forms broadly inhibit the ability of dendritic cells to fulfill their role as antigen-presenting cells.

KEYWORDS pneumocystis, T cells, cytokines, dendritic cells, fungal infection, lung defense

Pneumocystis species are opportunistic fungal pathogens that cause severe pneumonia in immunocompromised hosts, including AIDS patients and patients undergoing immunosuppressive therapies. Clearance of *Pneumocystis* organisms is dependent on the generation of effective CD4$^+$ T cell responses (1–3). Failure to clear *Pneumocystis* organisms leads to severe immune-mediated alveolar damage (4). While improvements in antiviral therapies have reduced the incidence of *Pneumocystis* pneumonia (PcP) in HIV-infected individuals and other at-risk populations, the mortality rate for patients with PcP has not improved (5). Additional studies are required to inform novel approaches to reduce morbidity and mortality due to *Pneumocystis* pneumonia.

Pneumocystis species have a biphasic life cycle consisting of trophic forms and cysts. Trophic forms are single-nucleated organisms typically found in clusters surrounded by

Received 5 June 2017 **Returned for modification** 23 June 2017 **Accepted** 4 July 2017

Accepted manuscript posted online 10 July 2017

Citation Evans HM, Simpson A, Shen S, Stromberg AJ, Pickett CL, Garvy BA. 2017. The trophic life cycle stage of the opportunistic fungal pathogen *Pneumocystis murina* hinders the ability of dendritic cells to stimulate CD4$^+$ T cell responses. Infect Immun 85:e00396-17. https://doi.org/10.1128/IAI.00396-17.

Editor Liise-anne Pirofski, Albert Einstein College of Medicine

Address correspondence to Beth A. Garvy, bgarv0@uky.edu.

* Present address: Shu Shen, Kelley Blue Book, Irvine, California, USA.

a biofilm-like substance consisting of a conglomeration of DNA, β-glucan, and other sugars (6). Cysts are ascus-like structures that consist of multiple nuclei surrounded by a fungal cell wall consisting of β-1,3-glucan and β-1,6-glucan (7–9). Trophic forms do not express β-glucan and do not form a cell wall (8).

Dendritic cells are the principal antigen-presenting cells in the lung. However, their role in initiating the adaptive response to *Pneumocystis* has been understudied. Previous work has demonstrated that dendritic cells activated by *Pneumocystis* cell wall-derived β-glucan increase the expression of costimulatory molecules and drive T_h1 polarization (10). The mechanism for dendritic cell recognition of *Pneumocystis* trophic forms, which do not express β-glucan, is unknown. Both stages express surface glycoproteins and mannoproteins that may serve as pathogen-associated molecular patterns (PAMPs) that could be recognized by receptors on host cells (7–9). Intriguingly, neither life form expresses the classical fungal components ergosterol, chitin, or α-glucan (10, 11).

We have previously reported that the life cycle stages of *Pneumocystis murina* have opposing effects on the immune response (11). The immune response to infection with *P. murina* trophic forms alone was less robust than the response to infection with a physiologically normal mixture of cysts and trophic forms. Infection with trophic forms alone resulted in reduced numbers of $CD11c^+$ innate immune cells in the lungs, as well as reduced recruitment of activated $CD4^+$ and $CD8^+$ T cells, compared to infection with a normal mixture of trophic forms and cysts. *In vitro*, trophic forms suppressed production of the proinflammatory cytokines interleukin-1β (IL-1β), IL-6, and tumor necrosis factor alpha (TNF-α) by bone marrow-derived dendritic cells (BMDCs) stimulated with β-glucan, zymosan, depleted zymosan, lipoteichoic acid (LTA), or lipopolysaccharides (LPS). In addition, trophic form-stimulated BMDCs failed to stimulate production of the T_h1-type cytokine gamma interferon (IFN-γ) by $CD4^+$ T cells.

Here, we demonstrate that *P. murina* trophic forms hinder the ability of dendritic cells to serve in their essential role as stimulators of $CD4^+$ T cell responses by reducing the capacity of dendritic cells to produce proinflammatory cytokines, present antigen, and express costimulatory molecules. Treatment of dendritic cells with trophic forms induced a less robust pattern of expression of immunity-related genes than treatment with a mixture of *P. murina* trophic forms and cysts. In addition, treatment with trophic forms reduced the ability of dendritic cells to increase surface expression of major histocompatibility complex (MHC) class II and CD40 in response to stimulation with mixed *P. murina* organisms or zymosan. These defects in the expression of MHC class II and costimulatory molecules corresponded with a reduced capacity for trophic form-loaded dendritic cells to stimulate $CD4^+$ T cell proliferation and polarization.

RESULTS

***P. murina* trophic forms induce a suppressive pattern of gene expression in dendritic cells.** *Pneumocystis* trophic forms suppress the production of proinflammatory cytokines by dendritic cells stimulated with multiple PAMPs (11). These PAMPs are recognized by a range of pattern recognition receptors that mediate diverse signaling pathways within the cell, including, in the case of IL-1β, inflammasome activation. These data suggest that *P. murina* trophic forms have a broadly suppressive effect on dendritic cells. To evaluate the activity of dendritic cells in response to trophic forms, we employed a target gene expression array to analyze the dendritic cell response to *P. murina* trophic forms based on the expression of 561 immunity-related mouse transcripts (NanoString nCounter Mouse Immunology CodeSet).

The normalized data illustrate that trophic forms induced a broader pattern of suppression in dendritic cells than stimulation with a normal mixture of cystic and trophic forms (mixed *Pneumocystis* organisms) or the β-glucan curdlan (Fig. 1A to D, mixed Pc or curdlan, respectively). Curdlan is a high-molecular-weight β-1,3-glucan isolated from *Alcaligenes faecalis* and is homologous to the β-1,3-glucan that composes the *P. murina* cyst wall (7, 8). Curdlan is employed in these experiments as a reductive positive control for β-glucan-induced signaling in BMDCs. The heat map shown in

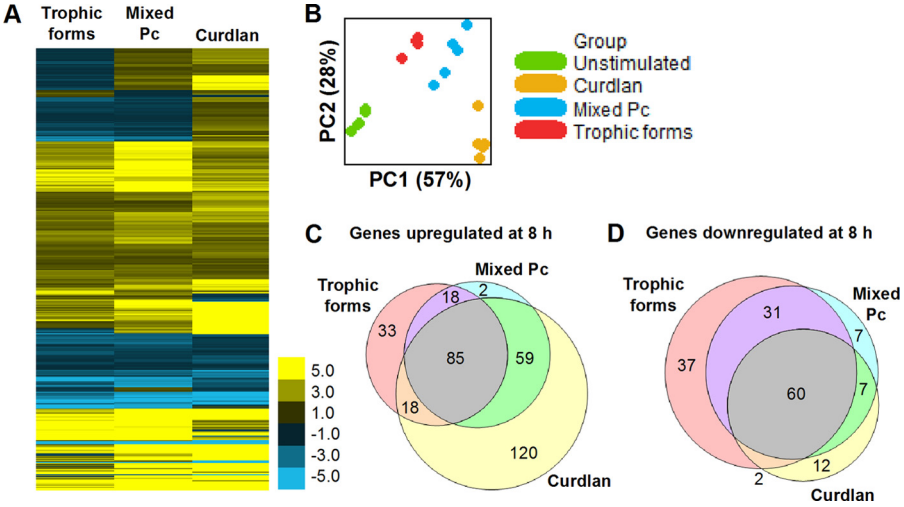

FIG 1 Exposure of BMDCs to *P. murina* trophic forms induces a distinct pattern of gene expression. A total of 3×10^5 BMDCs from adult BALB/cJ mice were incubated with 1.5×10^6 trophic forms or 1.5×10^6 mixed *P. murina* organisms (mixed Pc). Controls included untreated BMDCs and BMDCs treated with 10 μg/ml of the β-glucan curdlan. Cells were lysed after 2, 4, or 8 h of incubation. RNA was extracted. Gene expression analysis was carried out using a preassembled NanoString CodeSet that measures expression of 561 immunity-related mouse transcripts (nCounter Mouse Immunology kit). Analysis and normalization of the raw NanoString data were conducted using nSolver Analysis Software, version 2.0. Raw counts were normalized to those of the internal positive controls and reference transcripts. A heat map (A) was generated to display the expression value in treated cells relative to that in untreated cells. Principal-component (PC) analysis (B) was used to compare the patterns of gene expression among the untreated and treated groups following 8 h of incubation. Genes upregulated (C) or downregulated (D) in the treated groups relative to levels in the untreated control were identified by log-transformed two-way ANOVA, followed by pairwise comparisons using the least significant difference method. Five biological replicates were used per group. A change was deemed significant if the *P* value was <0.01.

Fig. 1A depicts the relative values of the 561 transcripts for each sample ($n = 5$) within each treatment group at 8 h posttreatment. Data are shown as the relative gene expression value compared to that of the unstimulated control. A large portion of the immunity-related genes were induced by treatment with curdlan but downregulated by treatment with trophic forms (Fig. 1A). Stimulation with a mixture of *P. murina* organisms did not induce total gene expression as robustly as treatment with the positive control, curdlan (Fig. 1A). However, stimulation with mixed *P. murina* organisms did lead to upregulation of a greater number of genes than stimulation with trophic forms alone (Fig. 1A). Intriguingly, stimulation with trophic forms and mixed *P. murina* organisms led to the upregulation of several genes whose expression was not induced by curdlan (Fig. 1A and C).

Experimental data shown in Fig. 1B represent the principal-component analysis-based clustering of the samples within each group after 8 h of treatment. Each of the groups formed distinct clusters, indicating a unique pattern of gene expression following each treatment. Experimental data shown in Fig. 1C and D represent genes upregulated or downregulated in the treated groups relative to levels in the untreated control ($P < 0.01$). Of the 561 immunity-related transcripts, stimulation with trophic forms induced the statistically significant upregulation of 154 genes (Fig. 1C) and the downregulation of 130 genes (Fig. 1D) relative to the levels in the unstimulated control. A total of 121/154 (78.6%) of the genes upregulated (Fig. 1C) by stimulation with trophic forms and 93/130 (71.5%) of the genes downregulated (Fig. 1D) by treatment with trophic forms were also upregulated or downregulated (respectively) in the mixed *P. murina*- and curdlan-treated groups. The pattern of gene expression in response to mixed *P. murina* organisms (a mixture of 10 trophic forms to one β-glucan-expressing cyst) was similar to the phenotypes induced by either trophic forms or curdlan, with few unique genes either up- or downregulated (Fig. 1C and D). The data shown in Fig. 1 demonstrate that trophic forms induce a unique pattern of gene expression in regard

to both the identity of the gene transcript and the magnitude of the change in expression. In contrast, treatment with mixed *P. murina* organisms induces a pattern of gene expression that represents an intermediate phenotype between the comparatively suppressive pattern of gene expression that is induced by trophic forms and the highly inflammatory pattern that is induced by the β-glucan curdlan.

Trophic forms induce the expression of genes encoding chemokines and complement proteins. As shown in Fig. 1C, stimulation with trophic forms induced the statistically significant upregulation of 154 genes compared to the levels in the unstimulated control. The data in Fig. S1A in the supplemental material represent genes in the NanoString panel with a statistically significant ($P < 0.01$) 4-fold or greater increase in expression in BMDCs treated with trophic forms compared to the level in unstimulated BMDCs. Several genes on this list are related to the complement system or encode chemokines. Notably, many of these genes, including the genes encoding complement system transcripts, are more highly expressed in cells treated with trophic forms than in cells stimulated with curdlan or a mixture of *P. murina* organisms.

The data in Fig. S1B and C represent all genes encoding regulators of inflammation or immunity-related transcription factors, respectively, with a statistically significant ($P < 0.01$) 2-fold or greater increase in expression in BMDCs treated with trophic forms compared to the level in unstimulated BMDCs. While we have previously reported that trophic forms fail to induce translocation of NF-κB in alveolar macrophages and that trophic forms suppress the production of IL-1β, IL-6, and TNF-α protein by dendritic cells, these data indicate that dendritic cells are responsive to the trophic forms (11, 12). Furthermore, treatment of dendritic cells with trophic forms induces a pattern of gene expression distinct from that of stimulation with curdlan and mixed *P. murina* organisms.

Stimulation with trophic forms leads to attenuated expression of multiple cytokine genes compared to treatment with a mixture of trophic forms and cysts. We previously published that *Pneumocystis* trophic forms suppressed the production of proinflammatory cytokines IL-1β, IL-6, and TNF-α by dendritic cells stimulated with multiple PAMPs (11). A principle aim of the gene expression array was to identify the extent of the suppressive impact of trophic forms on dendritic cells. Data shown in Fig. 2A represent relative gene expression at 8 h poststimulation of every cytokine included in the preassembled panel. Gene expression is displayed as the log2 value of the quotient of the value in treated cells divided by that in untreated cells. Stimulation with trophic forms led to the expression of the vast majority of the cytokine genes included in the panel. However, the magnitude of this upregulation was attenuated compared to treatment with mixed *P. murina* organisms or curdlan. For example, treatment with trophic forms increased the expression of transcripts encoding IL-1β and IL-6. However, this upregulation was not as great as that observed in cells stimulated with mixed *P. murina* organisms or curdlan (Fig. 2A). In addition, IL-1β and IL-6 proteins were not detectable in the supernatant of dendritic cells stimulated with purified trophic forms (Fig. S2). Treatment with trophic forms failed to induce gene and protein expression of TNF-α (Fig. 2A and S2). Mixed *P. murina* organisms and curdlan both induced expression of the transcript encoding TNF-α. However, as previously reported, stimulation with curdlan but not mixed *P. murina* organisms induced protein expression of TNF-α (11).

Trophic forms induce less robust expression of multiple transcription factors and positive regulators of inflammation than treatment with a mixture of trophic forms and cysts. Data shown in Fig. 2B represent genes that encode positive regulators of inflammation whose expression was significantly different (greater than 2-fold difference; $P < 0.01$) between the cells treated with trophic forms and those treated with mixed *P. murina* organisms at 8 h. Notably, treatment with trophic forms in the absence of cysts led to less robust expression of a wide range of mediators of inflammation, including the genes encoding the dendritic cell maturation marker SLAMF1, than stimulation with a mixed population of trophic forms and cysts. Data shown in Fig. 2C represent genes that encode immunity-associated transcription

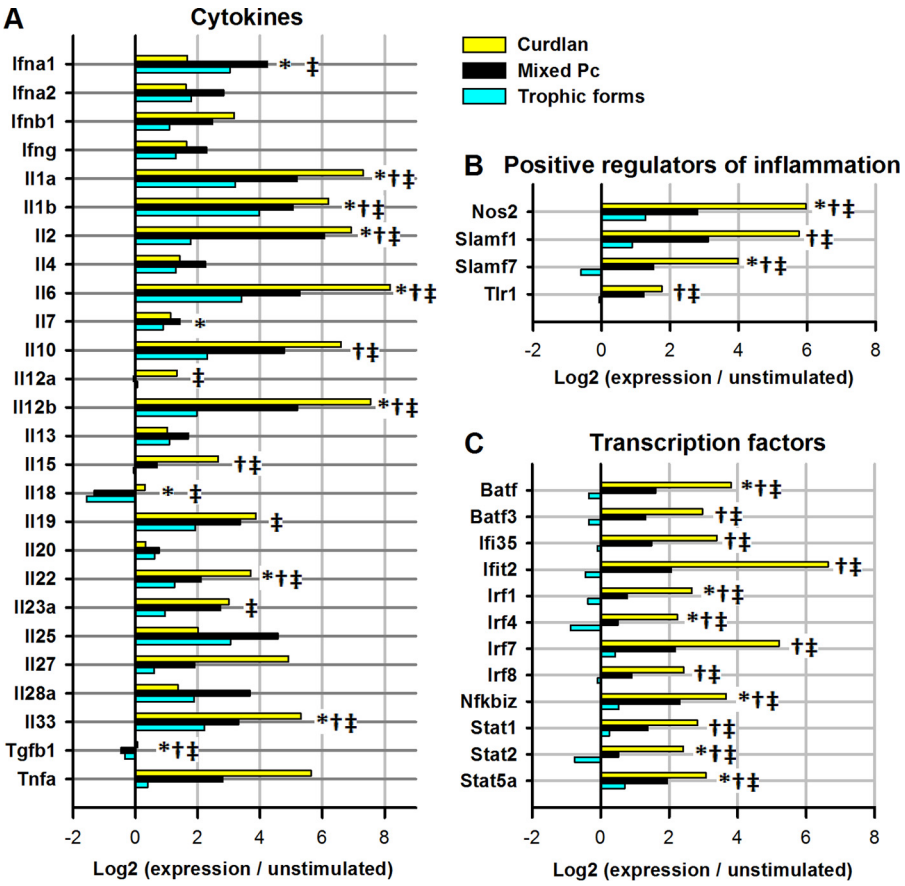

FIG 2 Trophic forms induce less robust expression of multiple cytokines, positive regulators of inflammation, and transcription factors than treatment with a mixture of trophic forms and cysts. The relative gene expression level after 8 h of treatment was calculated as the log2 value of the quotient of the expression value in treated cells divided by that of untreated cells. All cytokine genes in the preassembled NanoString panel are graphed (A). The data in panels B and C represent all genes encoding regulators of inflammation or immunity-related transcription factors with a statistically significant 2-fold or greater difference in expression between BMDCs treated with trophic forms versus those treated mixed *P. murina* organisms. Differences in expression levels between the groups were identified by log-transformed two-way ANOVA, followed by pairwise comparisons using the least significant difference method. Five biological replicates were used per group. A change was deemed significant if the *P* value was <0.01. Significant differences ($P < 0.01$) between results are indicated as follows: *, between BMDCs treated with trophic forms and unstimulated cells; †, between cells treated with trophic forms and those treated with mixed *P. murina* organisms; ‡, between cells treated with trophic forms and those treated with curdlan.

factors whose expression was significantly different (greater than 2-fold difference; $P < 0.01$) between the cells treated with trophic forms and those treated with mixed *P. murina* organisms at 8 h. Conventional dendritic cells (cDCs) may be divided into two broad subsets: CD8α^+ CD103$^+$ cDC1s, which promote T_h1 polarization, and CD11b$^+$ cDC2s, which promote T_h2 or T_h17-type responses (13–18). Treatment with trophic forms reduced the expression of the transcripts encoding the cDC1-associated transcription factors Batf3 and Irf8 and the expression of the cDC2-associated transcription factor Irf4 below the basal level of expression. In contrast, stimulation with mixed *P. murina* organisms enhances the expression of each of these markers.

Suppression of the cytokine response is not dependent on trophic form viability but is partially dependent on direct contact between trophic forms and dendritic cells. *Pneumocystis* trophic forms suppress the production of proinflammatory cytokines IL-1β, IL-6, and TNF-α by dendritic cells stimulated with multiple PAMPs (Fig. S2) (11). We report here that trophic forms are capable of suppressing the expression of multiple immunity-related genes (Fig. 1 and 2) below the basal level of expression. To determine if suppression requires live participation by the trophic forms,

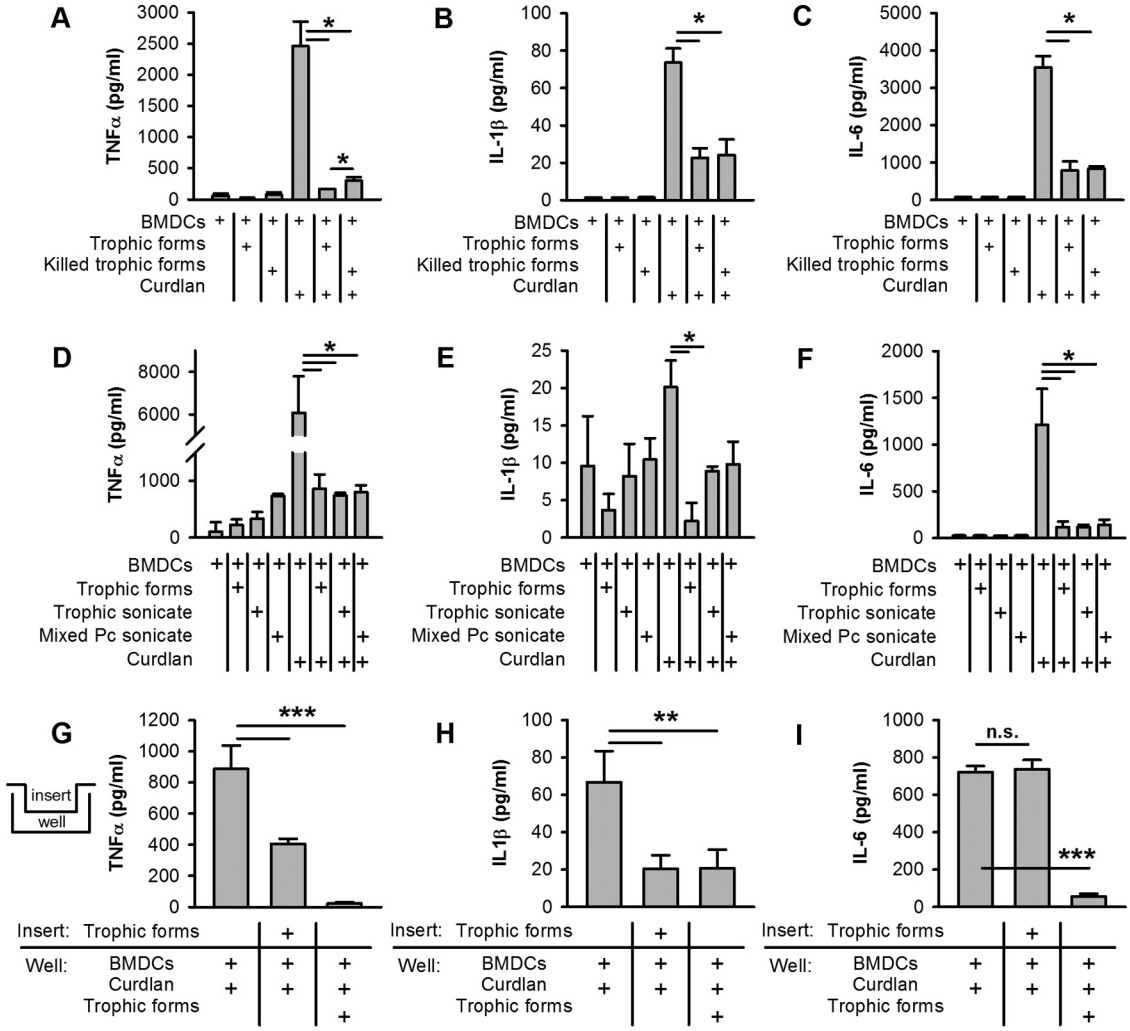

FIG 3 Suppression of the cytokine response is not dependent on trophic form viability but is partially dependent on direct contact between trophic forms and dendritic cells. A total of 1×10^4 BMDCs (A to F) from BALB/cJ mice were incubated with 5×10^5 trophic forms, 5×10^5 heat-killed trophic forms, 5×10^5 sonicated trophic forms, 5×10^5 sonicated mixed *P. murina* organisms, and/or 10 μg/ml curdlan for 72 h. A total of 1×10^5 BMDCs (G to I) from BALB/cJ mice were incubated with 5×10^6 trophic forms and/or 10 μg/ml curdlan for 72 h in a Transwell culture plate. TNF-α, IL-1β, and IL-6 cytokine production, as indicated, was quantified by ELISA. Data represent the means $\pm$ standard deviations of three biological replicates per group and are representative of two separate experiments. One-way ANOVA with Student-Newman-Keuls *post hoc* tests was used to compare differences among the groups where the data were parametric (A to D and G to I): *, $P \leq 0.05$; **, $P \leq 0.01$; ***, $P \leq 0.001$; n.s., not statistically significant. Kruskal-Wallis one-way ANOVA on ranks was used to compare differences among the groups where the data were nonparametric (E to F): *, $P \leq 0.05$.

we tested the ability of heat-killed (Fig. 3A to C) or sonicated (Fig. 3D to F) trophic forms to prevent IL-1β, IL-6, and TNF-α cytokine production in BMDCs treated with curdlan. Live, heat-killed, and sonicated trophic forms suppressed cytokine production, indicating that trophic-form-mediated suppression is not dependent on the viability of trophic forms. Surprisingly, while intact mixed *P. murina* organisms induce IL-1β and IL-6 production, these data indicate that sonicated mixed *P. murina* organisms suppressed these responses. These data suggest that intact cysts are required for stimulation of cytokine production, and, in the absence of this stimulation, that the trophic material is able to suppress the response to other PAMPs.

Immunosuppression by the trophic forms could be mediated by a secreted factor or by direct contact between the trophic forms and the BMDCs. We measured curdlan-induced IL-1β, IL-6, and TNF-α cytokine production by BMDCs separate from trophic forms by Transwell polyester inserts with 0.4-μm pores (Fig. 3G to I). Direct contact between the trophic forms and BMDCs was not required for a reduction in IL-1β or

TNF-α cytokine production (Fig. 3G and H). Intriguingly, direct contact was required for the suppression of IL-6 protein production (Fig. 3I).

A relatively small amount of *P. murina* DNA was detected in the lower Transwell compartment, and quantitative PCR indicated that up to 2×10^3 trophic forms (or equivalent trophic DNA) may have crossed the Transwell membrane (data not shown). However, the addition of greater than 10^6 trophic forms was required to see the level of suppression that was observed in the Transwell system (Fig. S3). In addition, a portion of the supernatant from the lower compartments was cytospun onto slides and examined under a microscope (limit of detection, 10^2 organisms) (data not shown). No trophic forms were observed, further confirming that a significant proportion of the trophic forms did not cross the membrane. These controls indicate that the suppression of TNF-α and IL-1β shown by the data in Fig. 3G to I was due to material secreted or shed from trophic forms rather than from the passage of whole trophic forms through the Transwell membrane.

Trophic forms suppress the expression of multiple factors related to antigen presentation, including MHC class II and the costimulatory molecule CD40. We have previously reported that infection of wild-type mice with trophic forms induces less expression of MHC class II on the surface of $CD11c^+$ $CD11b^-$ and $CD11c^+$ $CD11b^+$ cells within the lungs than infection with mixed *P. murina* organisms (11). This finding correlated with less robust $CD4^+$ T cell recruitment and proliferation in the lungs of mice infected with trophic forms than in mice infected with mixed *P. murina* organisms (11). The preassembled NanoString panel included several genes related to antigen presentation (Fig. 4A). These data indicate that trophic forms suppress the expression of multiple antigen presentation genes below the basal level of expression. *Ciita* encodes the class II transactivator, a master regulator of genes related to MHC class II expression. The expression of *Ciita* is 10-fold lower in BMDCs treated with trophic forms than in the unstimulated control (Fig. 4A). In contrast, stimulation with mixed *P. murina* organisms led to a 3-fold decrease in *Ciita* expression compared to the level in the unstimulated control, while treatment with curdlan did not significantly alter the expression of *Ciita* (Fig. 4A). Data shown in Fig. 4B represent the relative expression levels of genes encoding costimulatory molecules. Treatment of BMDCs with trophic forms induces lower levels of expression of the transcripts encoding the costimulatory molecules CD40, CD80, CD86, PD-L1, and PD-L2 than stimulation with mixed *P. murina* organisms.

Flow cytometry was used to evaluate protein expression of MHC class II (Fig. 4C and E) and CD40 (Fig. 4D and F) on the surface of BMDCs treated for 24 h with trophic forms, mixed *P. murina* organisms, and/or zymosan. Zymosan is a protein-carbohydrate preparation from the cell wall of *Saccharomyces cerevisiae*, and, unlike curdlan, zymosan may be processed and presented as protein antigen. Treatment of BMDCs with trophic forms resulted in reduced surface expression of MHC class II and CD40 compared to that after treatment with mixed *P. murina* organisms and/or zymosan. Addition of trophic forms to BMDCs treated with *P. murina* organisms or zymosan inhibited the expression of MHC class II and CD40 (Fig. 4E and F). These data indicate that trophic forms suppress the expression of MHC class II and the costimulatory molecule CD40 on the surface of dendritic cells. Maturation of dendritic cells is characterized by an initial burst in antigen presentation and MHC class II expression, followed by a reduction in additional antigen processing and presentation. However, surface expression of peptide-MHC class II complexes is highly stable in mature dendritic cells, with a reported half-life of 31 h observed in dendritic cells stimulated with LPS (19). Therefore, the observed reduction in MHC class II surface expression after 24 h of stimulation suggests that treatment with trophic forms impedes the maturation of dendritic cells.

Pretreatment of dendritic cells with trophic forms reduces allogeneic $CD4^+$ T cell proliferation in a mixed lymphocyte reaction. In order to determine the significance of reduced MHC class II on BMDCs treated with trophic forms, a mixed-lymphocyte reaction was used in which T cell proliferation is dependent on detection of allogeneic MHC class II but not specific antigen. To test the effect of trophic forms

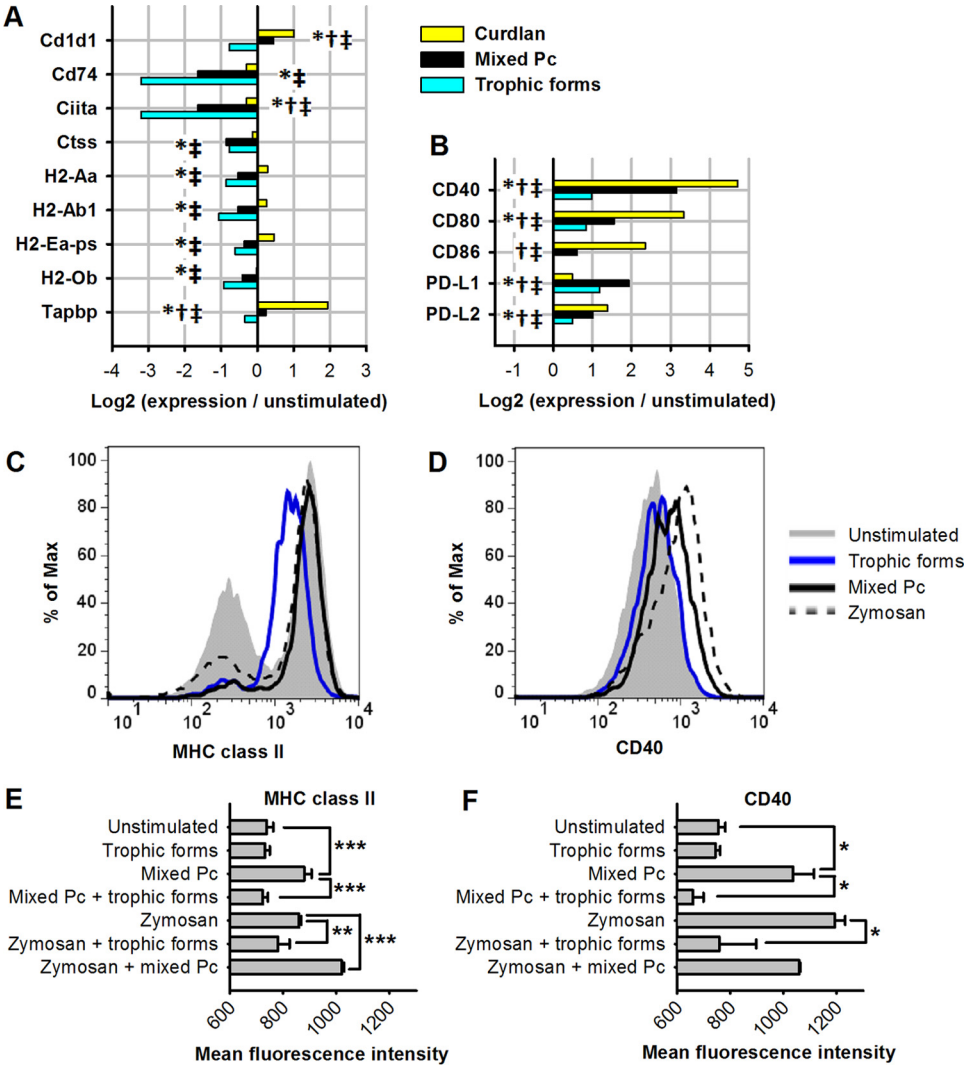

FIG 4 Trophic forms suppress the expression of multiple factors related to antigen presentation, including MHC class II and the costimulatory molecule CD40. The data in panels A and B represent genes in the NanoString panel encoding transcripts related to antigen-processing and presentation (A) or costimulatory molecules (B) with a statistically significant ($P < 0.01$) 2-fold or greater increase in expression in BMDCs treated with trophic forms compared to levels in unstimulated BMDCs. The relative gene expression after 8 h of treatment was calculated as the log2 value of the quotient of the expression value of treated cells divided by that of the untreated cells. Significant differences ($P < 0.01$) between results are indicated as follows: *, between BMDCs treated with trophic forms and unstimulated cells; †, between cells treated with trophic forms and cells treated with mixed *P. murina* organisms; ‡, between cells treated with trophic forms and those treated with curdlan. Flow cytometry was used to evaluate surface expression of MHC class II (C and E) and CD40 (D and F) on the surface of BMDCs following 24 h of treatment with trophic forms, mixed *P. murina* organisms, and/or the fungal cell wall preparation zymosan. Flow cytometry data represent the means ± standard deviations of three biological replicates per group and are representative of two separate experiments. One-way ANOVA with Student-Newman-Keuls *post hoc* tests was used to compare the surface expression of MHC class II or CD40 protein among the groups: *, $P \leq 0.05$; **, $P \leq 0.01$; ***, $P \leq 0.001$.

on allogeneic CD4$^+$ T cell proliferation, BMDCs generated from IA^d-expressing BALB/cJ mice were pretreated with trophic forms or mixed *P. murina* organisms for 1 h (Fig. 5A). Carboxyfluorescein succinimidyl ester (CFSE)-stained splenocytes from uninfected IA^b-expressing C57BL/6 mice were then added to the wells and cocultured for 6 days. Flow cytometry was used to evaluate the proliferation of C57BL/6 CD4$^+$ T cells (Fig. 5A). Pretreatment of allogeneic BMDCs with trophic forms, but not with mixed *P. murina* organisms, reduced CD4$^+$ T cell proliferation and IFN-γ production in the mixed-lymphocyte reaction (Fig. 5A). These data are consistent with trophic forms suppressing MHC class II expression, resulting in the inability of the pretreated dendritic cells to

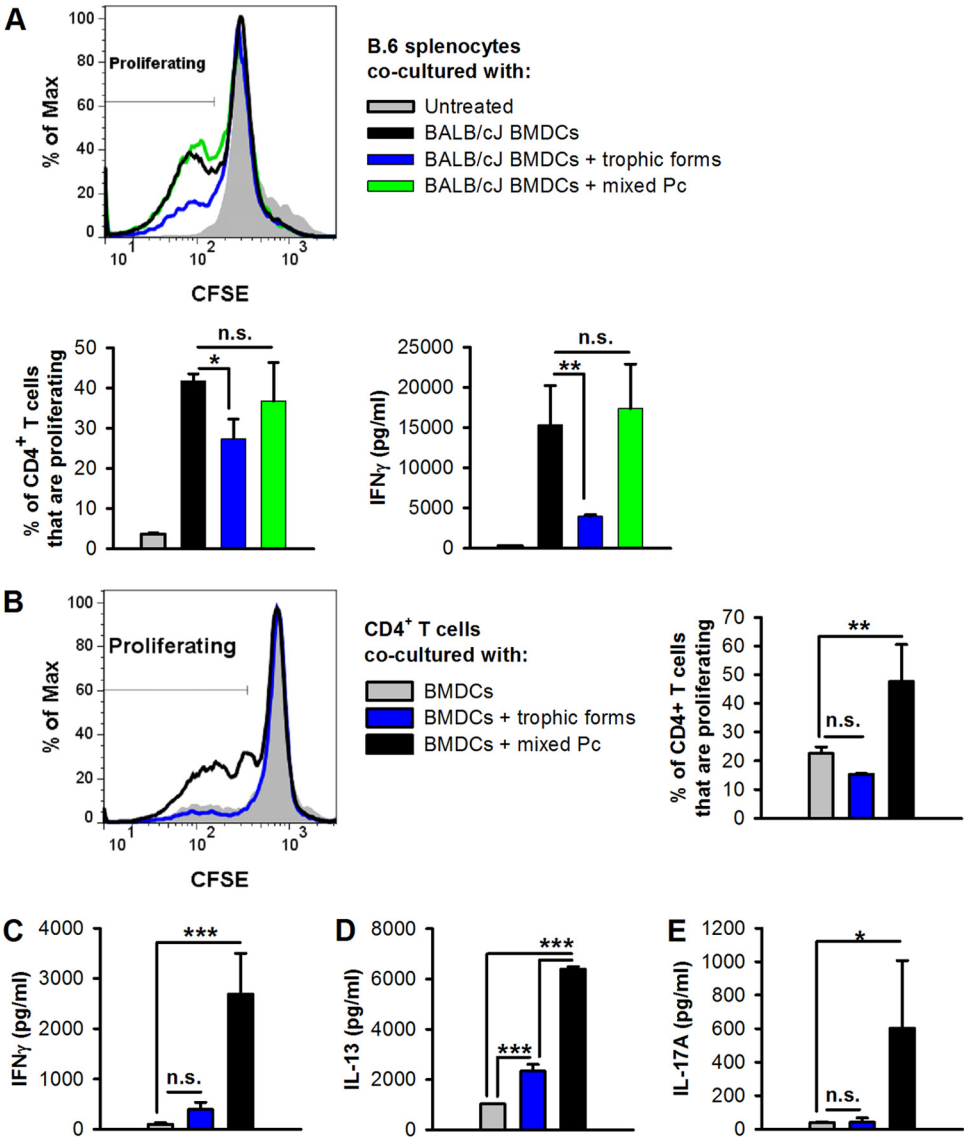

FIG 5 Trophic forms reduce dendritic cell-dependent proliferation of CD4$^+$ T cells. Treatment with trophic forms reduces CD4$^+$ T cell proliferation in response to coculture with allogeneic BMDCs in a mixed-lymphocyte reaction. (A) BMDCs generated from BALB/cJ mice were pretreated with trophic forms or mixed *P. murina* organisms for 1 h. CFSE-stained splenocytes from uninfected C57BL/6 mice were then added to the wells and cocultured for 6 days. Flow cytometry was used to identify the CD4$^+$ T cells and evaluate their proliferation. (B to E) BMDCs stimulated with trophic forms induce less proliferation and cytokine protein expression in CD4$^+$ T cells than cells stimulated with mixed *P. murina* organisms. BMDCs and CFSE-stained CD4$^+$ T cells from adult BALB/cJ mice were incubated with trophic forms or mixed *P. murina* organisms for 6 days. Flow cytometry was used to evaluate proliferation of CD4$^+$ T cells (B). ELISA was used to evaluate the concentrations of the cytokines IFN-γ (A and C), IL-13 (D), and IL-17A (E) in the supernatant. Data represent the means ± standard deviations of three biological replicates per group and are representative of at least two separate experiments. One-way ANOVA with Student-Newman-Keuls *post hoc* test was used to compare the percentage of proliferating CD4$^+$ T cells or supernatant cytokine concentration among the groups: *, $P \leq 0.05$; **, $P \leq 0.01$; ***, $P \leq 0.001$; n.s., not statistically significant.

stimulate antigen-independent allogeneic T cell proliferation in a mixed-lymphocyte reaction.

Trophic form-loaded dendritic cells stimulate less-robust CD4$^+$ T cell responses. CD4$^+$ T cell responses are required for the clearance of *P. murina* (2). We have previously reported that BMDCs loaded with mixed *P. murina* organisms, but not trophic forms, stimulate IFN-γ production by CD4$^+$ T cells *in vitro* (11). To evaluate whether dendritic cells are able to present antigen and induce CD4$^+$ T cell responses when loaded with trophic forms, we broadened our analysis to include proliferation

and other T helper cytokines (Fig. 5B to E). BMDCs loaded with mixed *P. murina* organisms, but not trophic forms, stimulated proliferation in CFSE-labeled $CD4^+$ T cells (Fig. 5B). To confirm that trophic forms are phagocytosed by BMDCs, confocal microscopy was used to demonstrate that 9-H-(1,3-dichloro-9,9-dimethylacridin-2-one-7-yl)-succinimidyl ester (DDAO-SE)-labeled trophic forms were internalized (Fig. S4A). Furthermore, confocal microscopy (Fig. S4B and C) and flow cytometry (Fig. S4D and E) confirmed that stimulation of dendritic cells with trophic forms does not reduce the ability of dendritic cells to phagocytose pHrodo green-labeled zymosan bioparticles, which fluoresce under low pH conditions.

BMDCs loaded with mixed *P. murina* organisms stimulated higher production of the T_h1-type cytokine IFN-γ, the T_h2-type cytokine IL-13, and the T_h17-type cytokine IL-17A by $CD4^+$ T cells than stimulation with trophic forms alone (Fig. 5C to E). However, stimulation with trophic forms did induce greater production of IL-13 than that of the unstimulated control (Fig. 5D). These data indicate that while cysts are required for robust proliferation of $CD4^+$ T cells and production of cytokines *in vitro*, BMDCs loaded with trophic forms are capable of driving modest T_h2-type T cell polarization. *P. murina* organisms did not stimulate $CD4^+$ T cell proliferation and cytokine production in the absence of BMDCs, indicating that these responses are dependent on antigen presentation by BMDCs (data not shown).

DISCUSSION

We have previously reported that the cyst life cycle stage drives proinflammatory responses that direct the early recruitment of innate and adaptive immune cells. Infection of adult mice with *Pneumocystis* trophic forms in the absence of cysts leads to the establishment of an immunosuppressive environment in the lungs that persists for up to 1 week following the formation of the cystic stage (11). If cysts are in the inoculum, the trophic form is unable to suppress inflammatory responses in the lungs as effectively. We have reported that the trophic life cycle forms dampen β-glucan and Toll-like receptor (TLR)-induced inflammation compared to the level after stimulation with a mixture of trophic forms and cysts (11). Here, our data confirm that *P. murina* trophic forms hinder the ability of dendritic cells to serve in their essential role as stimulators of $CD4^+$ T cell responses by reducing the capacity of dendritic cells to produce proinflammatory cytokines, present MHC class II, and express costimulatory molecules.

We did not define the factor(s) expressed by the trophic forms that induces suppression. However, experiments were presented that have begun to define the nature of these factors. Intriguingly, suppression of the dendritic cell cytokine response was not dependent on trophic form viability and was only partially dependent on direct contact between trophic forms and dendritic cells. Not much is known about secreted proteins from *Pneumocystis* organisms, but it has been shown that the organisms can form a biofilm-like substance consisting of a conglomeration of carbohydrates and glycosylated proteins, including glycoprotein A (gpA; or major surface glycoprotein, MSG), presumably shed from the cell surface (6). It is plausible that either secreted proteins or shed glycosylated proteins such as gpA are responsible for trophic form-mediated suppression. This is an area of great interest and focus in our laboratory.

Dendritic cell activation is dependent on the expression of a wide range of transcription factors and signaling mediators related to inflammatory responses. Here, we report that trophic forms induced a differential pattern of gene expression in dendritic cells compared to that following treatment with a normal mixture of trophic forms and cysts. Treatment of dendritic cells with trophic forms induced a less robust pattern of expression of several immunity-related genes than treatment with a mixture of *P. murina* trophic forms and cysts. We previously published that *Pneumocystis* trophic forms suppressed the production of proinflammatory cytokines IL-1β, IL-6, and TNF-α by dendritic cells stimulated with multiple PAMPs, including β-glucan, LPS, LTA, zymosan, and depleted zymosan (11). Here, we demonstrate that transcript levels of these proinflammatory cytokines are lower in dendritic cells treated with trophic forms than

in those treated with mixed *P. murina* organisms. These data suggest that the cyst life cycle is required for robust cytokine production by dendritic cells.

Trophic forms induce differential regulation of several genes related to inflammation and transcription compared to levels with stimulation with mixed *P. murina* organisms. These genes encompass diverse signaling pathways, including genes encoding members of the interferon regulatory factor (IRF) and STAT families. Here, we show that treatment with trophic forms suppressed the expression of Batf3 and Irf8, which mediate the development of T_h1-promoting CD8α^+ CD103$^+$ conventional DCs (cDC1s). The expression of Irf4, which mediates the development of T_h2/T_h17-promoting CD11b$^+$ cDCs (cDC2s) was also suppressed by treatment with trophic forms but induced by treatment with mixed *P. murina* organisms. These data suggest that trophic forms may broadly suppress the development of multiple dendritic cell subsets and are consistent with the failure of trophic form-stimulated dendritic cells to induce robust production of T helper cytokines compared to that following stimulation with mixed *P. murina* organisms. It should be noted, however, that the BMDCs employed in these experiments more closely resemble monocyte-derived dendritic cells and are not true conventional dendritic cells, which require Flt3L for differentiation (20, 21). The ability of trophic forms to suppress Batf3, Irf8, and Irf4 expression in Flt3L-dependent conventional dendritic cells has not been evaluated.

Some fungal pathogens, including *Candida* spp. and *Histoplasma capsulatum*, may prevent phagosomal maturation and acidification (22–24). However, our data indicate that stimulation with trophic forms or mixed *P. murina* organisms does not reduce the phagocytic capacity of the dendritic cell. Rather, our data confirm that treatment with trophic forms reduces the ability of dendritic cells to present antigen. Treatment with trophic forms reduced the ability of dendritic cells to increase surface expression of MHC class II and CD40 in response to stimulation with mixed *P. murina* organisms or zymosan (a *Saccharomyces* cell wall preparation). Our data indicate that this suppression occurred at the level of transcription as treatment with trophic forms led to downregulation of several genes associated with MHC class II processing and expression, including the gene encoding the master class II transactivator, CIITA. Treatment with trophic forms also resulted in lower expression of the genes encoding the costimulatory molecules CD40, CD80, and CD86, as well as the immune regulatory molecules PD-L1, and PD-L2, than treatment with a mixture of organisms that contained cysts. These defects in the expression of MHC class II and costimulatory molecules corresponded with a reduced capacity for trophic form-loaded dendritic cells to stimulate CD4$^+$ T cell proliferation and polarization.

Modulation of the T helper phenotype of the inflammatory response is a common strategy employed by infectious fungi for immune evasion (25, 26). However, while T_h1 or T_h17 responses are critical for control of many fungal infections, a mixed T helper response is observed in response to *Pneumocystis* infection. This mixed response appears to be largely redundant as T_h1-, T_h2-, and T_h17-type responses have each been associated with clearance of *P. murina* organisms (27–32). Broad suppression of cytokine production by trophic forms may be necessary to overcome this redundancy and delay the activation of adaptive immunity against *P. murina*.

Here, the data indicate that dendritic cells loaded with trophic forms stimulate production of the T_h2-type cytokine IL-13 but not production of the T_h1-type cytokine IFN-γ or the T_h17-type cytokine IL-17A. These data indicate that trophic forms may polarize the immune response toward a weak T_h2-type response. However, the effectiveness of this response in the absence of CD4$^+$ T cell proliferation is unclear. In addition, it is unclear how trophic forms, which suppress IL-6 protein production (11) and fail to induce expression of the genes encoding IL-2, IL-4, and IL-13 as robustly as stimulation with mixed *P. murina* organisms, promote T_h2 polarization. The CD4$^+$ T cells used in this experiment were generated from the draining lymph nodes of donor mice infected with mixed *P. murina* organisms. We expect that this population included *P. murina*-specific T_h2 CD4$^+$ T cells (29, 31), which may have continued to produce IL-13 but not proliferate in the presence of trophic form-loaded dendritic cells. The failure of

trophic forms to induce T_h1 and T_h17 $CD4^+$ T cell polarization is consistent with the attenuated expression of the genes encoding IL-1β, IL-2, IL-6, and IL-12β compared to that with stimulation with mixed *P. murina* organisms.

In addition, trophic forms induce the expression of the genes that encode the transcription factors T-bet (*Tbx21*) and Gata3 (see Fig. S1C in the supplemental material), which mediate T_h1 and T_h2-type responses, respectively. T-bet expression in dendritic cells is required for effective polarization of T_h1 T cells (33–35). GATA3 expression in BMDCs is required for production of the T_h2-type cytokines IL-13 and IL-5 (36). This indicates that the failure of trophic forms to induce robust T_h1 and T_h2 responses is not due to direct suppression of the transcription of these master regulators.

Tolerogenic dendritic cells promote anergic or regulatory T cell responses by secreting IL-10, transforming growth factor β (TGF-β), and IL-2 and by expressing the inhibitory molecules PD-L1 and PD-L2. However, our data indicate that treatment of dendritic cells with trophic forms results in lower levels of gene expression of each of these tolerogenic markers than those produced by treatment with a mixture of trophic forms and cysts. Therefore, trophic forms are not likely to induce a classical tolerogenic phenotype in dendritic cells. Rather, our data indicate that treatment with trophic forms broadly reduces the ability of the dendritic cell to provide activation signals to the $CD4^+$ T cells.

The inflammatory potential of the cysts in the face of a 10-fold excess of suppressive trophic forms should not be understated. The ability of trophic forms to suppress cytokine production is dose dependent, and our data suggest that slight changes in the ratio of trophic forms to cysts may shift the balance between suppression and stimulation (11). Increasing the trophic form-to-cyst ratio from 10:1 to 12:1 (by the addition of 10^5 trophic forms) is sufficient for the trophic forms to begin to reduce the IL-6 response to the mixed population (11). Cysts are the transmittable life cycle stage during natural infection. Our *in vivo* data indicate that the cyst burden remains low during the first week postinfection but that cysts in the inoculum drive the initial inflammation (11). Therefore, the rapid establishment of an immunosuppressive trophic population may be critical to avoid preemptive detection and clearance in immunocompetent hosts. Conversely, immunocompromised mice with severe pneumonia experience a final burst of trophic growth in which the ratio of trophic forms to cysts reaches as high as 30:1 (unpublished observation). This population shift may prolong the life of the immunocompromised host by dampening inflammation and may extend the window of opportunity for the transmission of cysts to additional hosts.

In summary, our data indicate that the trophic life cycle stage of *Pneumocystis* limits the ability of dendritic cells to stimulate $CD4^+$ T cell polarization and proliferation by reducing the expression of MHC class II, costimulatory molecules, and proinflammatory cytokines. These defects may be traced back to reduced levels of gene expression of each of these factors compared to levels in dendritic cells stimulated with a physiologically normal mixture of trophic forms and cysts. We propose that the suppression of immune responses by the trophic forms promotes the colonization of *Pneumocystis* in immunocompetent hosts. This differential immune response to *Pneumocystis* trophic forms and cysts is most certainly a leading contributor to the success of the organisms as human pathogens.

MATERIALS AND METHODS

Mice. Six-week-old female BALB/cJ and C57BL/6 mice were purchased from the Jackson Laboratory and infected at 8 weeks of age for either the adult experiments or to generate $CD4^+$ T cells for the *in vitro* experiments. Uninfected adult female BALB/cJ and C57BL/6 mice from the Jackson Laboratory were used to generate BMDCs for the *in vitro* experiments. Mice were maintained at the University of Kentucky Department of Laboratory Animal Resources (DLAR) under specific-pathogen-free conditions. C.129S6(B6)-$Rag2^{tm1Fwa}$ N12 ($Rag2^{-/-}$) mice, originally from Taconic (Germantown, NY), were used to maintain a source of *P. murina* and were bred at DLAR in sterile microisolator cages with sterilized food and water. The University of Kentucky Institutional Animal Care and Use Committee approved all protocols regarding animal use.

***P. murina* isolation and infection.** Lungs were excised from *P. murina*-infected Rag2$^{-/-}$ mice and pushed through stainless steel mesh in Hanks' balanced salt solution (HBSS) containing 0.5% glutathione at pH 7.3, as previously described (11). Cell debris was broken up by aspiration through 20- and 26-gauge needles and then removed by centrifugation at 100 $\times$ *g* for 3 min. Trophic forms were isolated by removing the supernatant following centrifugation at 400 $\times$ *g* for 7 min. This preparation results in greater than 99% pure trophic forms (11). The pellet from the spin at 400 $\times$ *g* contained a mixed population of cysts and trophic forms at a typical ratio of 10:1 trophic forms to cysts. Erythrocytes in the pellet were lysed with water, and organisms were suspended in an equal volume of 2$\times$ phosphate-buffered saline (PBS). Organisms were incubated with 200 U of DNase (Sigma-Aldrich, St. Louis, MO) at 37°C for 30 min. Clumps were broken up by aspiration through a 26-gauge needle. The remaining cell debris was removed by centrifugation at 100 $\times$ *g* for 3 min, followed by passage over a 70-μm-pore-size filter. Aliquots of mixed *P. murina* organisms or purified trophic forms were diluted, and 100-μl aliquots were spun onto a 28.3-mm^2 area of glass slides. Slides were fixed in methanol and stained with DiffQuik (Siemens Healthcare Diagnostics, Inc., Deerfield, IL). Organism numbers were determined microscopically using a 100$\times$ oil immersion objective of a Nikon microscope.

Generation of murine cells for *in vitro* assays. BMDCs were generated from uninfected BALB/cJ and C57BL/6 adult female mice, as previously described (11). Briefly, BMDCs were produced by flushing cells from the bone marrow of the tibias and femurs of female adult mice with PBS plus 5% heat-inactivated fetal bovine serum (FBS). Erythrocytes were removed using ammonium chloride-potassium (ACK) lysing buffer (37). Cells were washed and resuspended in culture medium containing RPMI medium with 10% heat-inactivated FBS, 0.5 mM 2-mercaptoethanol, 1% minimal essential medium (MEM) with nonessential amino acids, 100 units/ml penicillin, 100 μg/ml streptomycin, and 50 μg/ml gentamicin. Cells were plated in 100-mm petri dishes at a cell density of 4 $\times$ 10^6 in 10 ml of culture medium with 20 ng/ml recombinant murine granulocyte-macrophage colony-stimulating factor (GM-CSF) (Peprotech, Rocky Hill, NJ). Plates were cultured at 37°C in 5.0% CO_2. An additional 10 ml of culture medium with 20 ng/ml recombinant murine GM-CSF was added to cells after 24 h of growth. Every 48 h thereafter, nonadherent cells were removed and replaced with 10 ml of fresh medium containing recombinant murine GM-CSF. Cells were cultured for 9 to 12 days. BMDCs were collected by vigorously washing plates with medium to remove loosely adherent cells. BMDCs were washed, resuspended, and split for phenotyping or cytokine assay. Greater than 80% of recovered cells were CD11c$^+$.

CD4$^+$ T cells were generated by infecting adult BALB/cJ mice with 10^7 mixed *P. murina* organisms as described previously. Tracheobronchial lymph nodes (TBLN) were excised 10 to 14 days postinfection and pushed through 70-μm-pore-size nylon mesh screens in HBSS. Erythrocytes were removed using ACK. Cells were washed and counted. CD4 (L3T4) microbeads were used for positive selection of CD4$^+$ cells (Miltenyi Biotec, San Diego, CA). Greater than 90% of recovered cells were CD4$^+$ T cells. Splenocytes for the mixed lymphocyte reaction were collected from uninfected adult C57BL/6 mice. Spleens were excised and pushed through 70-μm-pore-size nylon mesh screens in HBSS. Erythrocytes were removed using ACK. Cells were washed and counted.

NanoString gene expression assay. A total of 3 $\times$ 10^4 BMDCs in 96-well Stripwell plates were stimulated with 10 μg/ml curdlan (β-1,3-glucan from *Alcaligenes faecalis*), 1.5 $\times$ 10^6 trophic forms, or 1.5 $\times$ 10^6 mixed *P. murina* organisms at 37°C in 5.0% CO_2 for 2, 4, and 8 h in BMDC culture medium. Additional controls, including BMDCs treated with curdlan and trophic forms, were allowed to incubate for 72 h. The control supernatants were screened for IL-1β, IL-6, and TNF-α cytokine production by enzyme-linked immunosorbent assay (ELISA) (eBioscience, San Diego CA).

At the conclusion of the 2-, 4-, and 8-h time points, the appropriate Stripwell segments were removed from the plate structure. Strips were washed once with PBS. Cells were lysed in TriReagent, and RNA was extracted with a Direct-zol RNA MiniPrep kit (Zymo Research, Irvine CA). The Direct-zol RNA MiniPrep kit permitted optimal hybridization of samples to the NanoString probes, presumably due to reduced contamination of chaotropic salts compared to that with other RNA extraction protocols.

Quality of the RNA was confirmed with a 2100 Bioanalyzer instrument (Agilent Technologies, Santa Clara, CA). More than 50% of the RNA fragments from each sample were larger than 300 bp, satisfying the quality requirements for NanoString. The RNA integrity number (RIN) for all samples was above 8.0. A total of 200 ng of each sample was sent to the Microarray Core at the University of Kentucky for NanoString processing. A NanoString nCounter Mouse Immunology kit (NanoString Technologies, Seattle, WA) was used to quantify the expression of 561 genes related to the murine immune response. Briefly, samples were hybridized to a panel of capture probes, and reporter probes were labeled with fluorescent barcodes. Hybridized samples were immobilized and aligned on the NanoString nCounter cartridge. Reporter probes were read using the nCounter Analysis System (NanoString Technologies, Seattle, WA), and counts were tabulated for each target transcript. Raw NanoString data are provided in Data Set S1 in the supplemental material.

Analysis and normalization of the raw gene expression data were conducted using nSolver Analysis Software, version 2.0 (NanoString Technologies, Seattle, WA). Raw counts were normalized to those of the internal positive controls and to those of the following housekeeping genes: Alas1, Eef1g, G6pdx, Gapdh, Gusb, Hprt, Oaz1, Polr1b, Polr2a, Ppia, Rpl19, Sdha, Tbp, and Tubb5. Heat maps and principal-component analysis were prepared with the nSolver Analysis Software, version 2.0.

***In vitro* phagocytosis assays.** BMDCs were labeled with 0.5 μM CFSE (Tonbo Biosciences, San Diego, CA) for 10 min at room temperature. Trophic forms and mixed *P. murina* organisms were labeled with 1 μM CellTrace Far Red DDAO-SE at 37°C for 7 min. A total of 10^5 CFSE-labeled BMDCs were preincubated in chamber slides for 1 h at 37°C in 5.0% CO_2 in BMDC culture medium. A total of 2 $\times$ 10^5 DDAO-SE-labeled trophic forms or 2 $\times$ 10^5 DDAO-SE-labeled mixed *P. murina* organisms were incubated with the

BMDCs for 60 min. Samples were washed three times in PBS, followed by fixation in 10% neutral buffered formalin for 10 min. Slides were washed in PBS, and coverslips were mounted with Prolong Gold. Slides were cured for 48 h at room temperature. Slides were examined using a Nikon A1RSi microscope and NIS-Elements software. A minimum of 100 cells were analyzed per group.

A total of 10^5 BMDCs were incubated in round-bottom polystyrene tubes or on chamber slides for 1 h at 37°C in 5.0% CO_2 in BMDC culture medium. A total of 2×10^5 DDAO-SE-labeled trophic forms, 2×10^5 DDAO-SE-labeled mixed *P. murina* organisms, and/or 100 μg/ml pHrodo green-labeled zymosan bioparticles (ThermoFisher Scientific, Waltham, MA) were incubated with the BMDCs for 60 min. Samples were washed three times in PBS. For confocal microscopy, chamber slides were fixed in 10% neutral buffered formalin for 10 min at room temperature. Slides were washed in PBS and treated with 300 nM 4′,6′-diamidino-2-phenylindole (DAPI) for 30 min. Slides were washed in PBS, and coverslips were mounted with Prolong Gold. Slides were cured for 48 h at room temperature. Slides were examined using a Nikon A1RSi microscope and NIS-Elements software. A minimum of 100 cells were analyzed per group. For flow cytometry, samples in round-bottom polystyrene tubes were washed twice in cold PBS. Samples were resuspended in 300 μl of cold HBSS. The phagocytic capacity of the cells was determined by flow cytometry using an LSRII flow cytometer (BD Biosciences, San Jose, CA). One thousand dendritic cell events were acquired and analyzed using FlowJo software (TreeStar, Ashland, OR).

***In vitro* MHC class II and CD40 assays.** A total of 10^5 BMDCs were stimulated with 20 μg/ml zymosan (*Saccharomyces cerevisiae* cell wall), 10^6 trophic forms, and/or 10^6 mixed *P. murina* organisms at 37°C in 5.0% CO_2 for 24 h in BMDC culture medium. Adherent cells were collected from the plate using TrypLE expression dissociation reagent. Cells were washed with PBS containing 0.1% bovine serum albumin and 0.02% NaN3 and stained with appropriate concentrations of fluorochrome-conjugated antibodies specific for innate immune cells (anti-CD11c clone N418, anti-IA^d clone AMS-32.1, and anti-CD40 clone 3/23). Antibodies were purchased from eBioscience (San Diego, CA) or BD Biosciences (San Jose, CA). Expression of these molecules on the surface of the cells was determined by multiparameter flow cytometry using an LSRII flow cytometer. One thousand $CD11c^+$ events were routinely acquired and analyzed using FlowJo software.

***In vitro* $CD4^+$ T cell proliferation and polarization assays.** A total of 10^5 BMDCs and/or 5×10^5 CFSE-labeled $CD4^+$ T cells were stimulated with 20 μg/ml zymosan (*Saccharomyces cerevisiae* cell wall), 5×10^5 trophic forms, and/or 5×10^5 mixed *P. murina* organisms at 37°C in 5.0% CO_2 for 6 days in BMDC culture medium. For the mixed-lymphocyte reaction, 10^5 BALB/cJ BMDCs were pretreated with 5×10^5 trophic forms or mixed *P. murina* organisms for 1 h at 37°C in 5.0% CO_2, followed by the addition of 5×10^5 CFSE-labeled C57BL/6 splenocytes and further incubation for 6 days. Medium was collected from the plates and spun at $400 \times g$ for 7 min to separate cells from the supernatant. Supernatant was stored at −80°C for use in IFN-γ, IL-13, and IL-17A cytokine ELISAs (eBioscience, San Diego CA). Adherent cells were collected from the plate using TrypLE Express dissociation reagent (ThermoFisher Scientific, Waltham, MA). Dissociated cells were combined with the cell pellet from the plate medium and washed in fresh culture medium.

Cells were washed in sterile PBS and stained with Fixable Viability Dye eFluor780 (eBioscience, San Diego, CA). Cells were washed with PBS containing 0.1% bovine serum albumin and 0.02% NaN3 (PBA) and stained with peridinin chlorophyll protein (PerCP)-efluor710-conjugated anti-CD4 clone GK1.5. Cells were washed with PBA and resuspended in 300 μl of HBSS. $CD4^+$ T cell proliferation was evaluated by multiparameter flow cytometry using an LSRII flow cytometer (BD Biosciences, San Jose, CA). One thousand lymphocyte events were routinely acquired and analyzed using FlowJo software (TreeStar, Ashland, OR).

Transwell contact assay. A total of 1×10^5 BMDCs, 10 μg/ml curdlan, and/or 5×10^6 trophic forms were plated in the upper or lower compartments of Transwell plates with a polyester membrane with 0.4-μm pores (Corning, Corning, NY). Plates were incubated at 37°C in 5.0% CO_2 for 72 h in BMDC culture medium. Cytokine levels were analyzed as described above. To confirm that trophic forms did not cross the membrane, samples were cytospun directly onto slides and DiffQuik stained, and 50 fields were screened.

Additional Transwell replicates were screened for *P. murina* DNA by quantitative PCR. Briefly, DNA was isolated from both the top and bottom compartments of the Transwell dishes using a QIAamp minikit (Qiagen, Hilden, Germany). Presence of trophic DNA was detected using primers designed to amplify a portion of the 18S rRNA gene of *P. murina*. Sequences of the primers are the following: forward, 5′-GGGCTTCTTAGAGGGACTGTTGG; reverse, 5′-CGTGCGGCCCAGAACATCTA (IDT, Coralville, IA). The control plasmid for quantification of *P. murina* DNA contains the region of the 18S rRNA gene amplified by these primers (GenScript USA, Inc., Piscataway, NJ). DNA was also isolated from 10^4, 10^5, and 10^6 *P. murina* trophic forms. The quantitative PCR amplification was performed with DNA samples in triplicate for 39 cycles of 95°C for 5 s and 57°C for 30 s using iTaq SYBR green reagent in a C1000 Thermal Cycler with a CFX96 real-time PCR detection system (Bio-Rad, Hercules, CA). The amount of trophic DNA calculated to have crossed from the Transwell insert to the bottom chamber would be equivalent to 2×10^3 organisms. *Pneumocystis* trophic forms reside in a biofilm-like substance consisting of a conglomeration of DNA, β-glucan, and other sugars (6). It is possible that the trophic DNA detected across the Transwell represents shed DNA rather than intact organisms.

The number of organisms required to suppress cytokine expression in the Transwell system was determined by incubating 1×10^5 BMDCs, 10 μg/ml curdlan, and increasing numbers of trophic forms (ranging from 10^3 to 10^6 organisms) in the lower compartments of Transwell plates. Plates were incubated at 37°C in 5.0% CO_2 for 72 h in BMDC culture medium. Cytokine levels were analyzed as described above.

Heat-killed trophic forms. Trophic forms were heat-killed by incubation at 56°C for 1 h. Nonviability of the organisms was confirmed by inoculation into immunocompromised Rag2$^{-/-}$ mice. A total of 10^4 BMDCs were stimulated with 10 μg/ml curdlan, 5×10^5 trophic forms, and/or 5×10^5 heat-killed trophic forms at 37°C in 5.0% CO_2 for 72 h in BMDC culture medium. IL-1β, IL-6, and TNF-α cytokine levels were analyzed as described above.

Statistical analysis. Analysis and normalization of the NanoString data were conducted using nSolver Analysis Software, version 2.0 (NanoString Technologies, Seattle, WA). Differences among the groups were identified by log-transformed two-way analysis of variance (ANOVA), followed by pairwise comparisons using the least significant difference method. Five biological replicates were used per group. A change was deemed significant if the P value was <0.01.

All other data were analyzed utilizing the SigmaStat statistical software package (SPSS, Inc., Chicago, IL). Student's t test or one-way analysis of variance (ANOVA) with Student-Newman-Keuls *post hoc* tests was used to determine differences between groups when the data were parametric. Kruskal-Wallis one-way ANOVA on ranks was used to analyze differences between groups when the data were nonparametric. Data were determined to be significantly different when the P value was <0.05.

SUPPLEMENTAL MATERIAL

Supplemental material for this article may be found at https://doi.org/10.1128/IAI.00396-17.

SUPPLEMENTAL FILE 1, PDF file, 0.4 MB.

SUPPLEMENTAL FILE 2, XLSX file, 0.7 MB.

ACKNOWLEDGMENTS

We thank Kuey-Chu Chen and Donna Wall of the University of Kentucky Microarray Core Facility and Melissa Hollifield and Robert Hayman IV for technical assistance.

REFERENCES

1. Roths JB, Marshall JD, Allen RD, Carlson GA, Sidman CL. 1990. Spontaneous *Pneumocystis carinii* pneumonia in immunodeficient mutant scid mice. Natural history and pathobiology. Am J Pathol 136:1173–1186.
2. Harmsen AG, Stankiewicz M. 1990. Requirement for CD4$^+$ cells in resistance to *Pneumocystis carinii* pneumonia in mice. J Exp Med 172:937–945. https://doi.org/10.1084/jem.172.3.937.
3. Roths JB, Sidman CL. 1992. Both immunity and hyperresponsiveness to *Pneumocystis carinii* result from transfer of CD4$^+$ but not CD8$^+$ T cells into severe combined immunodeficiency mice. J Clin Invest 90:673–678. https://doi.org/10.1172/JCI115910.
4. Limper AH, Offord KP, Smith TF, Martin WJ, 2nd. 1989. *Pneumocystis carinii* pneumonia. Differences in lung parasite number and inflammation in patients with and without AIDS. Am Rev Respir Dis 140:1204–1209.
5. Miller RF, Allen E, Copas A, Singer M, Edwards SG. 2006. Improved survival for HIV infected patients with severe *Pneumocystis jirovecii* pneumonia is independent of highly active antiretroviral therapy. Thorax 61:716–721. https://doi.org/10.1136/thx.2005.055905.
6. Cushion MT, Collins MS, Linke MJ. 2009. Biofilm formation by *Pneumocystis* spp. Eukaryot Cell 8:197–206. https://doi.org/10.1128/EC.00202-08.
7. Matsumoto Y, Matsuda S, Tegoshi T. 1989. Yeast glucan in the cyst wall of *Pneumocystis carinii*. J Protozool 36:21S–22S. https://doi.org/10.1111/j.1550-7408.1989.tb05814.x.
8. Nollstadt KH, Powles MA, Fujioka H, Aikawa M, Schmatz DM. 1994. Use of beta-1,3-glucan-specific antibody to study the cyst wall of *Pneumocystis carinii* and effects of pneumocandin B0 analog L-733,560. Antimicrob Agents Chemother 38:2258–2265. https://doi.org/10.1128/AAC.38.10.2258.
9. Kottom TJ, Hebrink DM, Jenson PE, Gudmundsson G, Limper AH. 2015. Evidence for proinflammatory β-1,6 glucans in the *Pneumocystis carinii* cell wall. Infect Immun 83:2816–2826. https://doi.org/10.1128/IAI.00196-15.
10. Carmona EM, Vassallo R, Vuk-Pavlovic Z, Standing JE, Kottom TJ, Limper AH. 2006. *Pneumocystis* cell wall beta-glucans induce dendritic cell costimulatory molecule expression and inflammatory activation through a Fas-Fas ligand mechanism. J Immunol 177:459–467. https://doi.org/10.4049/jimmunol.177.1.459.
11. Evans HM, Bryant GL, III, Garvy BA. 2016. The life cycle stages of *Pneumocystis murina* have opposing effects on the immune response to this opportunistic, fungal pathogen. Infect Immun 84:3195–3205. https://doi.org/10.1128/IAI.00519-16.
12. Kurkjian C, Hollifield M, Lines JL, Rogosky A, Empey KM, Qureshi M, Brown SA, Garvy BA. 2012. Alveolar macrophages in neonatal mice are inherently unresponsive to *Pneumocystis murina* infection. Infect Immun 80:2835–2846. https://doi.org/10.1128/IAI.05707-11.
13. Edelson BT, Kc W, Juang R, Kohyama M, Benoit LA, Klekotka PA, Moon C, Albring JC, Ise W, Michael DG, Bhattacharya D, Stappenbeck TS, Holtzman MJ, Sung SS, Murphy TL, Hildner K, Murphy KM. 2010. Peripheral CD103$^+$ dendritic cells form a unified subset developmentally related to CD8α^+ conventional dendritic cells. J Exp Med 207:823–836. https://doi.org/10.1084/jem.20091627.
14. Hildner K, Edelson BT, Purtha WE, Diamond M, Matsushita H, Kohyama M, Calderon B, Schraml BU, Unanue ER, Diamond MS, Schreiber RD, Murphy TL, Murphy KM. 2008. Batf3 deficiency reveals a critical role for CD8α^+ dendritic cells in cytotoxic T cell immunity. Science 322:1097–1100. https://doi.org/10.1126/science.1164206.
15. Schlitzer A, Ginhoux F. 2014. Organization of the mouse and human DC network. Curr Opin Immunol 26:90–99. https://doi.org/10.1016/j.coi.2013.11.002.
16. Merad M, Sathe P, Helft J, Miller J, Mortha A. 2013. The dendritic cell lineage: ontogeny and function of dendritic cells and their subsets in the steady state and the inflamed setting. Annu Rev Immunol 31:563–604. https://doi.org/10.1146/annurev-immunol-020711-074950.
17. Schlitzer A, McGovern N, Teo P, Zelante T, Atarashi K, Low D, Ho AW, See P, Shin A, Wasan PS, Hoeffel G, Malleret B, Heiseke A, Chew S, Jardine L, Purvis HA, Hilkens CM, Tam J, Poidinger M, Stanley ER, Krug AB, Renia L, Sivasankar B, Ng LG, Collin M, Ricciardi-Castagnoli P, Honda K, Haniffa M, Ginhoux F. 2013. IRF4 transcription factor-dependent CD11b$^+$ dendritic cells in human and mouse control mucosal IL-17 cytokine responses. Immunity 38:970–983. https://doi.org/10.1016/j.immuni.2013.04.011.
18. Plantinga M, Guilliams M, Vanheerswynghels M, Deswarte K, Branco-Madeira F, Toussaint W, Vanhoutte L, Neyt K, Killeen N, Malissen B, Hammad H, Lambrecht BN. 2013. Conventional and monocyte-derived CD11b$^+$ dendritic cells initiate and maintain T helper 2 cell-mediated immunity to house dust mite allergen. Immunity 38:322–335. https://doi.org/10.1016/j.immuni.2012.10.016.
19. Simmons DP, Wearsch PA, Canaday DH, Meyerson HJ, Liu YC, Wang Y, Boom WH, Harding CV. 2012. Type I IFN drives a distinctive dendritic cell maturation phenotype that allows continued class II MHC synthesis and antigen processing. J Immunol 188:3116–3126. https://doi.org/10.4049/jimmunol.1101313.
20. Xu Y, Zhan Y, Lew AM, Naik SH, Kershaw MH. 2007. Differential devel-

opment of murine dendritic cells by GM-CSF versus Flt3 ligand has implications for inflammation and trafficking. J Immunol 179:7577–7584. https://doi.org/10.4049/jimmunol.179.11.7577.
21. Mayer CT, Ghorbani P, Nandan A, Dudek M, Arnold-Schrauf C, Hesse C, Berod L, Stuve P, Puttur F, Merad M, Sparwasser T. 2014. Selective and efficient generation of functional Batf3-dependent CD103$^+$ dendritic cells from mouse bone marrow. Blood 124:3081–3091. https://doi.org/10.1182/blood-2013-12-545772.
22. Eissenberg LG, Goldman WE, Schlesinger PH. 1993. *Histoplasma capsulatum* modulates the acidification of phagolysosomes. J Exp Med 177:1605–1611. https://doi.org/10.1084/jem.177.6.1605.
23. Marcil A, Gadoury C, Ash J, Zhang J, Nantel A, Whiteway M. 2008. Analysis of PRA1 and its relationship to *Candida albicans*-macrophage interactions. Infect Immun 76:4345–4358. https://doi.org/10.1128/IAI.00588-07.
24. Seider K, Brunke S, Schild L, Jablonowski N, Wilson D, Majer O, Barz D, Haas A, Kuchler K, Schaller M, Hube B. 2011. The facultative intracellular pathogen *Candida glabrata* subverts macrophage cytokine production and phagolysosome maturation. J Immunol 187:3072–3086. https://doi.org/10.4049/jimmunol.1003730.
25. Chai LY, Netea MG, Vonk AG, Kullberg BJ. 2009. Fungal strategies for overcoming host innate immune response. Med Mycol 47:227–236. https://doi.org/10.1080/13693780802209082.
26. Romani L. 1999. Immunity to *Candida albicans*: Th1, Th2 cells and beyond. Curr Opin Microbiol 2:363–367. https://doi.org/10.1016/S1369-5274(99)80064-2.
27. Fraser IP, Takahashi K, Koziel H, Fardin B, Harmsen A, Ezekowitz RA. 2000. *Pneumocystis carinii* enhances soluble mannose receptor production by macrophages. Microbes Infect 2:1305–1310. https://doi.org/10.1016/S1286-4579(00)01283-1.
28. Garvy BA, Wiley JA, Gigliotti F, Harmsen AG. 1997. Protection against *Pneumocystis carinii* pneumonia by antibodies generated from either T helper 1 or T helper 2 responses. Infect Immun 65:5052–5056.
29. Shellito JE, Tate C, Ruan S, Kolls J. 2000. Murine CD4$^+$ T lymphocyte subsets and host defense against *Pneumocystis carinii*. J Infect Dis 181:2011–2017. https://doi.org/10.1086/315487.
30. Rudner XL, Happel KI, Young EA, Shellito JE. 2007. Interleukin-23 (IL-23)-IL-17 cytokine axis in murine *Pneumocystis carinii* infection. Infect Immun 75:3055–3061. https://doi.org/10.1128/IAI.01329-06.
31. Myers RC, Dunaway CW, Nelson MP, Trevor JL, Morris A, Steele C. 2013. STAT4-dependent and -independent Th2 responses correlate with protective immunity against lung infection with *Pneumocystis murina*. J Immunol 190:6287–6294. https://doi.org/10.4049/jimmunol.1300431.
32. Linke MJ, Ashbaugh A, Collins MS, Lynch K, Cushion MT. 2013. Characterization of a distinct host response profile to *Pneumocystis murina* asci during clearance of *pneumocystis* pneumonia. Infect Immun 81:984–995. https://doi.org/10.1128/IAI.01181-12.
33. Lugo-Villarino G, Maldonado-Lopez R, Possemato R, Penaranda C, Glimcher LH. 2003. T-bet is required for optimal production of IFN-gamma and antigen-specific T cell activation by dendritic cells. Proc Natl Acad Sci U S A 100:7749–7754. https://doi.org/10.1073/pnas.1332767100.
34. Lugo-Villarino G, Ito S, Klinman DM, Glimcher LH. 2005. The adjuvant activity of CpG DNA requires T-bet expression in dendritic cells. Proc Natl Acad Sci U S A 102:13248–13253. https://doi.org/10.1073/pnas.0506638102.
35. Heckman KL, Radhakrishnan S, Peikert T, Iijima K, McGregor HC, Bell MP, Kita H, Pease LR. 2008. T-bet expression by dendritic cells is required for the repolarization of allergic airway inflammation. Eur J Immunol 38:2464–2474. https://doi.org/10.1002/eji.200737952.
36. Yashiro T, Kubo M, Ogawa H, Okumura K, Nishiyama C. 2015. PU.1 suppresses Th2 cytokine expression via silencing of GATA3 transcription in dendritic cells. PLoS One 10:e0137699. https://doi.org/10.1371/journal.pone.0137699.
37. Harding CV, Canaday D, Ramachandra L. 2010. Choosing and preparing antigen-presenting cells. Curr Protoc Immunol Chapter 16:Unit 16.1. https://doi.org/10.1002/0471142735.im1601s88.